Published online August 2, 2004

4060–4070 *Nucleic Acids Research, 2004, Vol. 32, No. 13*
doi:10.1093/nar/gkh743

Enhanced nucleic acid binding to ATP-bound hepatitis C virus NS3 helicase at low pH activates RNA unwinding

Angela M. I. Lam, Ryan S. Rypma and David N. Frick*

Department of Biochemistry and Molecular Biology, New York Medical College, Valhalla, NY 10595, USA

Received June 11, 2004; Revised and Accepted July 15, 2004

ABSTRACT

The molecular basis of the low-pH activation of the helicase encoded by the hepatitis C virus (HCV) was examined using either a full-length NS3 protein/NS4A cofactor complex or truncated NS3 proteins lacking the protease domain, which were isolated from three different viral genotypes. All proteins unwound RNA and DNA best at pH 6.5, which demonstrate that conserved NS3 helicase domain amino acids are responsible for low-pH enzyme activation. DNA unwinding was less sensitive to pH changes than RNA unwinding. Both the turnover rate of ATP hydrolysis and the K_m of ATP were similar between pH 6 and 10, but the concentration of nucleic acid needed to stimulate ATP hydrolysis decreased almost 50-fold when the pH was lowered from 7.5 to 6.5. In direct-binding experiments, HCV helicase bound DNA weakly at high pH only in the presence of the non-hydrolyzable ATP analog, ADP(BeF_3). These data suggest that a low-pH environment might be required for efficient HCV RNA translation or replication, and support a model in which an acidic residue rotates toward the RNA backbone upon ATP binding repelling nucleic acid from the binding cleft.

INTRODUCTION

Hepatitis C virus (HCV) non-structural protein 3 (NS3) is a multifunctional enzyme with two distinct activities (1). The N-terminal portion of NS3 is a serine protease involved in viral polyprotein processing, and the C-terminal NS3 portion is an RNA helicase with possible roles in translation and viral RNA synthesis. Since both these activities are critical for HCV replication (2), the NS3 protein has been studied in depth as a target for rational antiviral drug design. Structural and mechanistic studies focusing on HCV NS3 has led to the development of the first specific HCV protease inhibitors currently in clinical trials (3). However, despite an abundance of data, precisely how the NS3 helicase moves along RNA or unwinds a double helix is still not clear.

The purpose of this study is to examine the effect of pH on HCV helicase. Several previous studies have indicated that HCV helicase might be most active at a low pH, and the nature of this activation could highlight key protein features critical for unwinding. Because NS3 is one of the best-studied members of a broad class of enzymes called DExH/D box proteins (4), which itself is only a small part of helicase superfamily 2 (5), the resulting insights could also help to explain how such proteins move along, unwind and re-arrange RNA molecules. Several proteins related to HCV helicase also have been reported to be most active at low pH, including the Rad3 helicase encoded by *Saccharomyces cerevisiae* (6). Rad3 is the yeast homolog of the human xeroderma pigmentosum group D (XPD) repair helicase that is part of the transcription factor IIH complex. Mutations in XPD have been linked to Xeroderma pigmentosum, Cockayne Syndrome and Trichothiodystrophy (7).

Numerous structural studies using X-ray crystallography (8–11) and NMR (12,13) have revealed that the portion of NS3 comprising the helicase forms a three-domain Y-shaped molecule. Only domains 1 and 2 are similar to those seen in other helicases, and they contain several conserved motifs characteristic of superfamily 2 helicases. Domain 3 is a novel domain composed primarily of α-helices. The HCV helicase likely unwinds a double helix by moving along one strand in a 3′ to 5′ direction while separating it from the complementary strand. ATP, which fuels strand separation, most likely binds in a cleft between domains 1 and 2, and one strand of the double helix binds in the cleft that separates domains 1 and 2 from domain 3 (9). In the absence of ATP, NS3 helicase tightly grips single-stranded RNA (ssRNA) (or DNA) with one key residue in domain 3, Trp-501, stacking like a bookend between nucleic acid bases (9). ATP binding appears to allosterically modulate the affinity of HCV helicase for nucleic acid so that the helicase releases RNA to move along the helix. Most present models speculate that the closure of the cleft between domains 1 and 2 upon ATP binding and its opening upon hydrolysis or ADP release allow HCV to move on RNA like an inchworm (9,14,15).

In support of the inchworm model, when the HCV helicase binds the non-hydrolyzable ATP analog ADP(BeF_3), it binds DNA weakly, but precisely how much weaker is still not clear. Whereas Levin *et al*. (15) reported that the HCV helicase binds ssDNA over 100-fold less tightly in the presence of ADP(BeF_3) (15), other studies using different recombinant NS3 proteins have observed only a 5–10-fold decrease in ssDNA affinity upon ADP(BeF_3) binding to HCV helicase

*To whom correspondence should be addressed. Tel: +1 914 594 4190; Fax: +1 914 594 4058; Email: David_Frick@NYMC.edu

(14,16). Below, we show that this apparent difference is due to the fact that the studies were performed at a different pH. Furthermore, we show that the increased affinity for ssDNA in the presence of ATP at low pH allows HCV helicase to unwind nucleic acids more rapidly at a low pH. This effect is more dramatic when RNA is used as a substrate, and consequently, RNA is only unwound at low pH whereas HCV helicase retains some DNA helicase activity at physiological pH. Because the NS3 protease domain and NS4A protease cofactor do not eliminate this low-pH requirement, the fact that HCV helicase requires an acidic environment to unwind RNA could have important implications in the viral life cycle.

MATERIALS AND METHODS

Reagents

RNAase-free reagents were purchased from Ambion Inc. (Austin, TX), and RNA oligonucleotides were from Dharmacon (Lafayette, CO). 3-(Cyclohexylamino)propane sulfonic acid (CAPS), *N*-Tris(hydroxymethyl)methylglycine (TRICINE), Tris, MOPS, PIPES and morpholinoethane sulfonic acid (MES) buffers were each prepared at the same ionic strength and treated with RNAsecure reagent (Ambion) prior to use. DNA oligonucleotides were obtained from Integrated DNA Technologies (Corralville, IA). Beryllium fluoride was from Alfa Aesar (Ward Hill, MA). The truncated NS3 helicases (His–Hel, Hel–His and His–Hel–His) were purified to apparent homogeneity as described previously (16,17). The purified full-length His–NS3–4A complex was a gift from Dr Baohua Gu (The Jefferson Center of Biomedical Research) and was purified as reported previously (16).

Unwinding assays

To generate substrates for helicase assays, two synthetic oligonucleotides were annealed by heating them to 95°C and allowing them to cool slowly to room temperature. Before annealing, the shorter strand was ^{32}P-labeled using polynucleotide kinase. The DNA substrate consisted of a shorter DNA oligonucleotide 5′-[^{32}P]GCC TCG CTG CCG TCG CCA-3′ annealed to a longer DNA oligonucleotide 5′-TGG CGA CGG CAG CGA GGC TTT TTT TTT TTT TTT TTT TT-3′. The duplex RNA substrate consisted of the RNA oligonucleotide 5′-[^{32}P]GCC UCG CUG CCG UCG CCA-3′ annealed to the oligonucleotide 5′-UGG CGA CGG CAG CGA GGC UUU UUU UUU UUU UUU UUU UU-3′. The DNA or RNA substrate (1 nM) and 100 nM HCV helicase were incubated in reaction buffer (25 mM buffer, 3 mM $MgCl_2$ and 0.1% Tween-20) for 15 min. Reactions were initiated by the addition of 5 mM ATP, terminated with EDTA and analyzed by non-denaturing PAGE as described previously (14,16,17).

Single turnover unwinding reactions were performed like the standard reactions except that 1 μM excess unlabeled short DNA oligonucleotide (5′-GCC TCG CTG CCG TCG CCA-3′) was added as an enzyme trap at reaction initiation. Data were fit to a pseudo-first-order rate equation to determine (k_{obs}) and reaction amplitude. In other words, the percentage of unwound DNA (%U) at various times (t) was fit to Equation 1 by non-linear regression.

$$\%U(t) = \text{Amplitude}\left(1 - e^{-k_{obs}t}\right). \quad \mathbf{1}$$

ATPase assay

Reactions were performed at 37°C in 25 mM buffer, 3 mM $MgCl_2$, 0.2% Tween-20, ATP at indicated concentrations and helicase. Data obtained in the absence of nucleic acids were fit to the Michaelis–Menten equation by non-linear regression to calculate K_m (basal) and k_{cat} (basal). Data obtained in the presence of 2 mM poly(U) RNA were fit to the Michaelis–Menten equation by non-linear regression to calculate K_m (stim.) and k_{cat} (stim.). To determine the constant K_{NA}, defined as the concentration of nucleic acids that supports a half maximum rate of catalysis, reactions were performed in the presence of 4 mM ATP with various concentrations of poly(U) RNA (average length 2500 nt) or dT20 DNA (5′-TTTTT TTTTT TTTTT TTTTT-3′). Data were fit to Equation 2, where v_o is the initial rate of ATP hydrolysis, [NA] is the nucleic acid concentration (expressed in total nucleotide concentration) and $[E]_T$ is the total enzyme concentration (expressed in moles of protein monomer).

$$\frac{v_o}{[E]_T} = \frac{k_{cat}^{stim.}[NA]}{K_{NA} + [NA]} + k_{cat}^{basal}. \quad \mathbf{2}$$

Fluorescence-based nucleic acid binding assay

Aliquots of DNA were added to the helicase in 2 ml of 25 mM MOPS at the indicated pH, 3 mM $MgCl_2$ and 0.2% Tween-20 at 25°C. Fluorescence was measured by exciting the sample at 280 nm and reading the emission at 340 nm with a Varian Carey Eclipse fluorescence spectrophotometer. After correcting data for dilution and inner filter effects, fractional fluorescence F_{NA} was calculated by dividing the fluorescence values by the initial fluorescence of the protein in the absence of DNA. F_{NA} was fit to the total concentration of added dT20 oligonucleotide ($[NA]_T$) using an equation accounting for ligand depletion:

$$F_{NA} = 1 - \Delta FF_{MAX}\frac{(K_D + [NA]_T + [E]_T) - \sqrt{(K_D + [NA]_T + [E]_T)^2 + 4[NA]_T[E]_T}}{2[E]_T}. \quad \mathbf{3}$$

In Equation 3, ΔFF_{MAX} is the maximum change in fractional fluorescence resulting when all enzyme molecules are bound to nucleic acid. K_D is the dissociation constant and $[E]_T$ is total enzyme concentration. The procedure was repeated at various pH for each enzyme/oligonucleotide pair both in the presence and absence of the non-hydrolyzable ATP analog, ADP(BeF_3), which was formed by including 0.1 mM ADP, 5 mM NaF and 0.5 mM BeF_2 in the reaction buffer (18). K_D was calculated by globally fitting datasets to Equation 3 using Graphpad Prism Version 4.0 (San Diego, CA). Note, because [NA] in Equation 3 is expressed in terms of oligonucleotide concentration (i.e. concentration of 3′ ends), whereas in Equation 2 [NA] is expressed in total nucleotide concentration (i.e. concentration of bases); the values for K_D obtained from Equation 3 are not directly comparable to K_{NA} values.

mantADP(BeF_3) binding assay

To analyze pH effects on ATP binding to HCV helicase, the formation of a 2′-*O*-(*N*-methylanthraniloyl)adenosine 5′-diphosphate (mantADP)–BeF_3–helicase complex was monitored using fluorescence resonance energy transfer (FRET) as described previously (15). A solution containing 0.5 μM Hel–His, 3 mM $MgCl_2$, 0.2% Tween-20, 25 mM MOPS-NaOH, 5 mM NaF and 0.5 mM BeF_2 was titrated with mantADP. FRET was monitored by exciting the sample at 280 nm and the emitted light was monitored at 443 nm. After subtracting background fluorescence in the absence of mantADP, the data were fit to Equation 4:

$$\mathrm{FRET} = F_F * \left\{ [A]_T - \left(\frac{(K_D + [A]_T + [E]_T) - \sqrt{(K_D + [A]_T + [E]_T)^2 + 4[A]_T[E]_T}}{2} \right) \right\} + F_C * \left(\frac{(K_D + [A]_T + [E]_T) - \sqrt{(K_D + [A]_T + [E]_T)^2 + 4[A]_T[E]_T}}{2} \right). \quad 4$$

In Equation 4, K_D is the dissociation constant for enzyme and mantADP, $[A]_T$ is total mantADP, $[E]_T$ is the total helicase, F_F is the fluorescence coefficient for free mantADP and F_C is the fluorescence coefficient for the mantADP(BeF_3)–helicase complex.

Magnesium binding assay

The FRET observed in a helicase–mantATP complex was also used to analyze the pH dependence of Mg^{2+} binding to HCV helicase. Solutions containing 0.5 μM Hel–His, 2 μM mantADP, 0.2% Tween-20, 25 mM MOPS-NaOH, 5 mM NaF and 0.5 mM BeF_2 were titrated with $MgCl_2$. Because magnesium concentrations far exceeded both enzyme and mantADP concentrations, dissociation constants for Mg^{2+} were calculated by fitting a plot of FRET versus magnesium concentration to Equation 5, where F_{max} is the maximum possible FRET and K_D is the dissociation constant.

$$\mathrm{FRET} = \frac{F_{max}[Mg^{2+}]}{K_D + [Mg^{2+}]}. \quad 5$$

RESULTS

Several research groups have reported that HCV helicase unwinds DNA and RNA most rapidly around pH 6.5 but functions markedly slower below pH 6 or above pH 7 (19–22). However, several other groups have reported that the HCV helicase works best at a more neutral pH (23,24). Similarly, whereas Suzich *et al*. (25) originally reported that ATP hydrolysis catalyzed by NS3 in the presence of poly(U) RNA peaks at pH 6.5, others have reported very different results (26,27). To clarify this situation, and more thoroughly analyze the effect of pH on HCV helicase, several different assays were performed with various buffers within their buffering capacity. The assays were repeated using either an NS3–NS4A complex (designated His–NS3–4A) or truncated NS3 proteins in which the protease was replaced by an N-terminal His-tag, designated (His–Hel and His–Hel–His) or a His-tagged helicase which lacks any remnant of the protease (Hel–His). The purification and characterization of these proteins were recently described in (16,17). The assays were performed with so many different proteins because we recently showed that the full-length protein with its NS4A cofactor unwinds RNA better than truncated versions (16), and it is possible that pH influences the full-length NS3 somewhat different from that has been reported previously. In addition, since the histidines used in the fusion tag could affect the results, the experiments were repeated using proteins in which the His-tag was placed in very different locations [for details see Figure 1 of (16)]. As a separate control, the His-tag was removed from His–NS3–4A using thrombin digestion. The

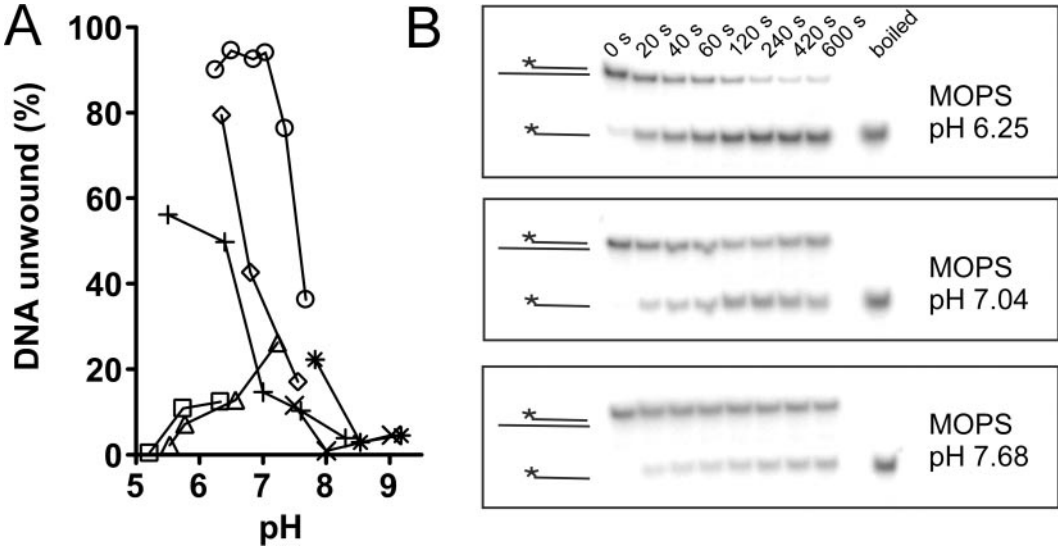

Figure 1. HCV helicase catalyzed DNA unwinding in various buffer systems. (**A**) 1 nM of a DNA substrate was incubated with 100 nM of HCV helicase (His–Hel) and 5 mM ATP for 10 min at 23°C in either citrate buffer (squares), MES-NaOH buffer (triangles), PIPES-NaOH buffer (diamonds), MOPS-NaOH buffer (circles), Tris–HCl buffer (×), Tris–Malate buffer (+) or Tricene-HCl (*). Data are reported as percent of substrate unwound. (**B**) Native polyacrylamide gels showing the time course of the reactions catalyzed in MOPS buffers at pH 6.25, 7.04 and 7.68. Reactions were terminated at various times are shown along with a boiled substrate control.

digested NS3–4A protein was then separated from the His-tag (and residual His–NS3–4A) using immobilized metal ion affinity chromatography. Although similar pH profiles were obtained with the NS3–4A protein, the resulting data are not reported here because the digested protein lost ~50% of its activity and appeared to be partially degraded.

In addition to the above proteins, which were all isolated from the H77c strain of HCV genotype 1a (16,17), the assays were repeated with analogous Hel–His proteins isolated from the genotype 1b HC-J4 [Hel–His (genotype 1b)] and the HCV genotype 2a infectious clone HC-J6 [Hel–His (genotype 2a)]. We wanted to determine if distinctive pH profiles are conserved properties because some variation in helicase activity has been observed among the HCV genotypes (17).

The first assays that were performed were designed to identify an appropriate buffer system to study the pH profile of the HCV helicase. In these experiments, DNA unwinding was observed under conditions where no re-annealing occurs (1 nM substrate and 100 nM helicase for 0–10 min at 23°C). DNA was used as a substrate initially because, in general, it is unwound faster than RNA by HCV helicase and thus provides a more sensitive assay. Typical results obtained for each recombinant HCV helicase protein are shown in Figure 1. The HCV helicase functions best near pH 6.5, and its activity rapidly decreases above pH 7. The protein is also buffer sensitive, and among the buffers tested, MOPS was clearly preferred. Since the MOPS buffers also span a biologically relevant pH range, from cellular pH to the pH of optimal activity, we decided to more rigorously analyze the activity of full-length HCV helicase (His–NS3–4A) and truncated NS3 containing only the helicase domain (His–Hel, Hel–His and His–Hel–His) in MOPS buffers.

Effect of pH on HCV NS3-mediated RNA unwinding

RNA unwinding was measured using a duplex RNA with a 3′ single-stranded poly(U) tail. Each assay contained 1 nM RNA substrate and 100 nM of either His–NS3–4A or His–Hel. Reactions were terminated at various times and the amounts of dissociated products were determined using non-denaturing PAGE. Under these conditions, no RNA re-annealing occurs because the excess enzyme molecules trap the dissociated strands (14). As was reported by others (19–22), both enzymes unwound RNA the fastest at pH 6.5, and unwinding rates fell rapidly when pH was lowered (in reactions in MES or PIPES buffers) or raised (in reactions in MOPS buffers).

Figure 2 shows that the HCV helicase is indeed a low-pH activated RNA helicase and that the residues responsible for this low-pH activation reside in the helicase portion of the NS3 protein. The full-length NS3–NS4A complex (His–NS3–4A) unwinds almost 30 times slower above pH 7.5, than at pH 6.5, and at pH 7.0 RNA is unwound 5 times slower than it is at pH 6.5 (Figure 2A). The NS3–4A protease appears to somewhat lessen the effect of pH on RNA unwinding. When the experiment in Figure 2A was repeated with His–Hel, the fastest rates of RNA unwinding were again observed at acidic pH (6.25–6.5), but this time almost no unwound RNA could be detected above pH 7.0 (Figure 2B). The ability of His–NS3–4A to unwind faster than His–Hel likely results from the ability of the protease domain to aid processive RNA unwinding (16).

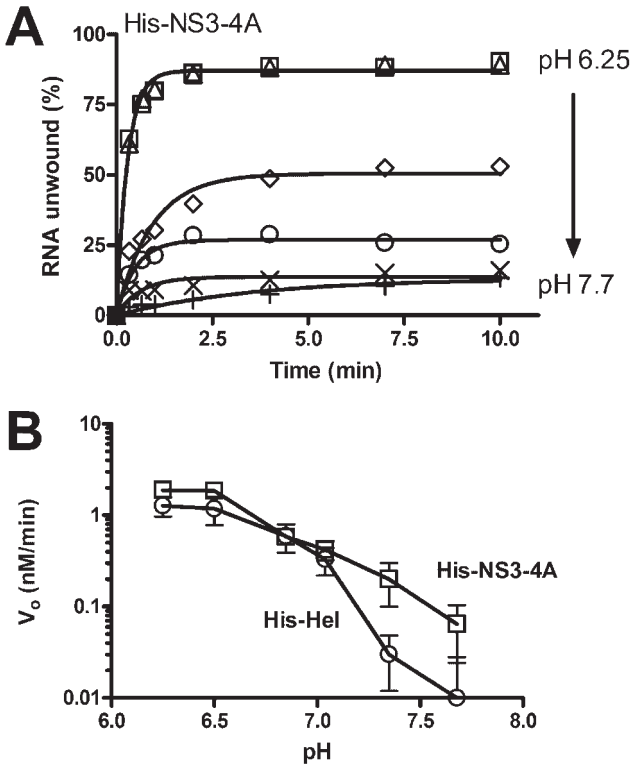

Figure 2. Effect of pH on HCV helicase catalyzed RNA unwinding. (**A**) Reactions containing the full-length HCV protease helicase complex (His–NS3–4A) were carried out in MOPS buffer at pH 6.25 (squares), pH 6.5 (triangles), pH 6.85 (diamonds), pH 7.04 (circles), pH 7.35 (×) and pH 7.68 (+). All reactions contained 1 nM of duplex [^{32}P]RNA substrate and 100 nM protein, were initiated with ATP, incubated at 37°C for various times, terminated and analyzed using native polyacrylamide gels. (**B**) Initial rates of RNA unwinding in reactions catalyzed by His–NS3–4A (squares) are compared with the rates of the same reactions catalyzed by His–Hel (circles). The average rates obtained from three separate reactions are shown with standard deviations as error bars.

DNA unwinding catalyzed by HCV NS3 is less sensitive to pH than RNA unwinding

Even though there is no known DNA stage in the replication cycle of HCV, it is well established that HCV helicase unwinds DNA better than the corresponding RNA duplex (14,17,28). In fact, at pH 6.5 (37°C), if DNA unwinding is measured using a DNA substrate bearing the same sequence as the RNA duplex (except with U's replacing T's), then the entire duplex would be unwound in <1 min (14,16). Therefore, to analyze the effect of pH on DNA unwinding, the reactions described in Figure 2 were repeated with a DNA duplex using the same MOPS buffers at 23°C, where the reaction is slower. When compared with RNA unwinding, DNA unwinding was also affected by pH but to a lesser extent (Figure 3). Again, the rate of unwinding was fastest in MOPS buffers and was at its peak between pH 6 and 6.85. Reactions performed with His–NS3–4A in MOPS buffers are shown in Figure 3A, and the same reactions with His–Hel are shown in Figure 3B. Increasing pH reduced DNA unwinding rates. However, at pH 7.68, His–Hel still unwound DNA at one-fourth the rate seen at the pH optimum (Figure 3B), whereas the more efficient His–NS3–4A retained ~50% of its activity (Figure 3A). An analysis of the initial reaction rates (Figure 3B) reveals that

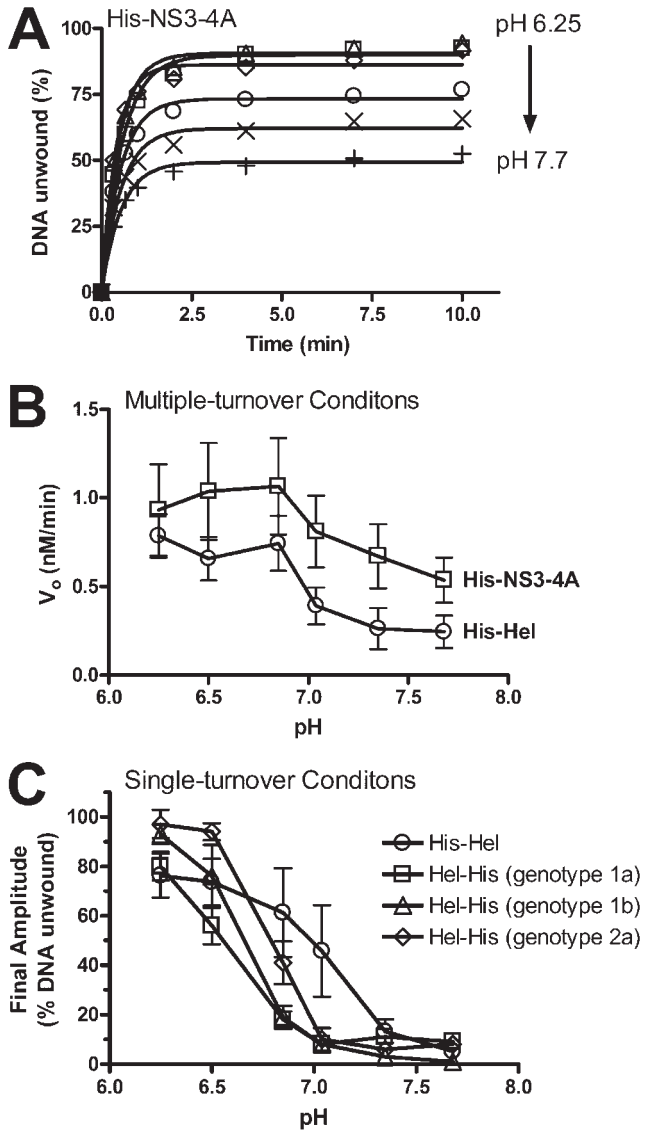

Figure 3. Effect of pH on HCV helicase catalyzed DNA unwinding. (**A**) Reactions containing His–NS3–4A were carried out in MOPS buffer at pH 6.25 (squares), pH 6.5 (triangles), pH 6.85 (diamonds), pH 7.04 (circles), pH 7.35 (x) and pH 7.68 (+). All reactions contained 1 nM of duplex [^{32}P]DNA substrate and 100 nM protein, were initiated with ATP, incubated at 23°C for various times, terminated and analyzed using native polyacrylamide gels. (**B**) Initial rates of DNA unwinding in reactions catalyzed by His–NS3–4A (squares) are compared with the same reactions catalyzed by His–Hel (circles) and plotted versus pH. The average rates obtained from three separate reactions are shown with the standard deviation as error bars. (**C**) DNA unwinding reactions were performed as above but in the presence of 1 μM of oligonucleotide that functions as an enzyme trap (single turnover conditions). Data were fit to Equation 1 to determine the final amplitudes of reactions catalyzed by His–Hel (circles) or Hel–His isolated from HCV genotype 1a (squares), genotype 1b (triangles) or genotype 2a (diamonds).

the optimal pH range for both proteins is from 6.25 to 6.85. As seen in RNA helicase assays, the pH profile of DNA unwinding catalyzed by His–NS3–4A and the pH profile of His–Hel catalyzed DNA unwinding are similar.

The above unwinding reactions were performed under conditions where the amount of enzyme greatly exceeded the amount of substrate. Such conditions were necessary because the excess enzyme traps displaced single-stranded oligonucleotides preventing them from re-annealing. In addition, if the enzyme falls from the substrate before unwinding is complete, then another enzyme can bind the substrate and complete the reaction. Thus, although these 'multiple-turnover' conditions provide a sensitive assay system, they could mask subtle differences in reaction rates. Therefore, the DNA unwinding reactions were repeated under 'single-turnover' conditions, where 1 μM of 'trap' oligonucleotide (with the same sequence as the shorter substrate strand, but lacking a radiolabel) was added at reaction initiation. The trap oligonucleotide acts to sequester excess enzyme that is not initially bound to the substrate when the reaction is started. These experiments were performed with His–NS3–4A, His–Hel and three different Hel–His enzymes isolated from three different HCV genotypes. The results of the single-turnover assays performed with His–Hel and the three Hel–His enzymes are shown in Figure 3C and demonstrate that DNA unwinding, like RNA unwinding is exquisitely sensitive to pH. When the data are fit to a first-order rate equation (Equation 1), the final reaction amplitude is clearly lower at higher pH (Figure 3C). Because helicases isolated from three different HCV genotypes behave similarly, this low-pH activated helicase activity appears to be evolutionarily conserved. Differences in final reaction amplitudes reached at different pH could result from either differences in ATP hydrolysis, ATP binding or DNA binding. These ideas are tested below.

Effect of pH on HCV NS3-mediated ATP hydrolysis

Because ATP hydrolysis catalyzed by HCV helicase fuels unwinding, one might reasonably expect that rates of ATP hydrolysis in the presence of RNA to depend on pH like the helicase activity. Some studies have previously reported such an effect (25,26), but other studies have reported that nucleic acid-stimulated ATP hydrolysis catalyzed by HCV helicase is less dependent on pH (21,22). Generally, most studies that measure the pH dependence of rates of HCV helicase catalyzed ATP hydrolysis in the absence of nucleic acids agree that basal ATPase rates are less pH sensitive than either RNA unwinding or nucleic acid-stimulated ATP hydrolysis (25,26).

The above studies suggest that ATP hydrolysis, like unwinding, might be low-pH activated, but the reason for this activation is unclear. The activation could be due to variation in one (or more) of the five steady-state kinetic parameters that describe helicase catalyzed ATP hydrolysis. The first two of these parameters, k_{cat} (basal) and K_m (basal), describe the turnover rate of ATP hydrolysis in the absence of nucleic acid and the concentration of ATP supporting half that rate. The second two parameters, k_{cat} (stim.) and K_m (stim.), are the first-order rate constant describing the maximum rate of nucleic acid-stimulated ATP hydrolysis and the concentration of ATP supporting half this maximum rate. The fifth kinetic constant, K_{NA}, is defined as the concentration of nucleic acid that supports half of the maximum rate of stimulated ATP hydrolysis. Using techniques described previously (17), we determined each of these constants in various buffer systems that covered the pH range from 5 to 10.

When ATPase assays were performed with either His–Hel, Hel–His or His–NS3–4A, similar pH profiles were again obtained with all three proteins. The results obtained with His–Hel are shown in Figure 4. The initial rates of

[γ-^{32}P]ATP hydrolysis by His–Hel were measured in reactions that contained various amounts of ATP. The data were fit to the Michaelis–Menten equation to obtain a basal K_m and a k_{cat}. In the absence of RNA or DNA (Figure 4A), HCV helicase hydrolyzed ATP at similar maximum rates between pH 6 and 10. Under these conditions, the turnover rate for His–Hel was between 2 and 4 s^{-1}, and the K_m for ATP ranged from 2 to 10 μM. The turnover rate for His–NS3–4A varied ~1.5 s^{-1}, with a K_m for ATP that ranged from 200 to 300 μM. Below pH 6, HCV helicase hydrolyzed ATP somewhat slower, and above pH 10 hydrolysis rates slowed considerably (Figure 4A).

When the same ATP titrations were repeated in the presence of saturating amounts (2 mM total nucleotide concentration) of poly(U) RNA (average length 2500 nt), His–Hel hydrolyzed ATP about 30 times faster (Figure 4B). Again, hydrolysis rates were similar between pH 6 and 10, with a k_{cat} of ~60 s^{-1} and a K_m that varies randomly from 200 to 400 μM. The full-length protein His–NS3–4A was stimulated less than His–Hel [as was reported previously (16)], but had a virtually identical pH profile as His–Hel. The first-order rate constant describing His–NS3–4A stimulated catalyzed ATP hydrolysis ranged from 10 to 15 s^{-1} and the K_m of ATP under stimulated conditions was consistently ~1.5 mM.

The data in Figure 4 show that HCV helicase catalyzed ATP hydrolysis is not pH-dependent in the same manner as RNA unwinding. Although k_{cat} (basal) almost doubled, k_{cat} (stim.) did not increase as pH was lowered from 7.5. However, very different results were obtained when ATPase assays were performed in the presence of sub-optimal levels of RNA (or DNA). Under such conditions, ATP hydrolysis was much faster at low pH because the rates of ATP hydrolysis were dependent not only on ATP binding, but also on nucleic acid binding. As shown in Figure 5, the parameter K_{NA}, which

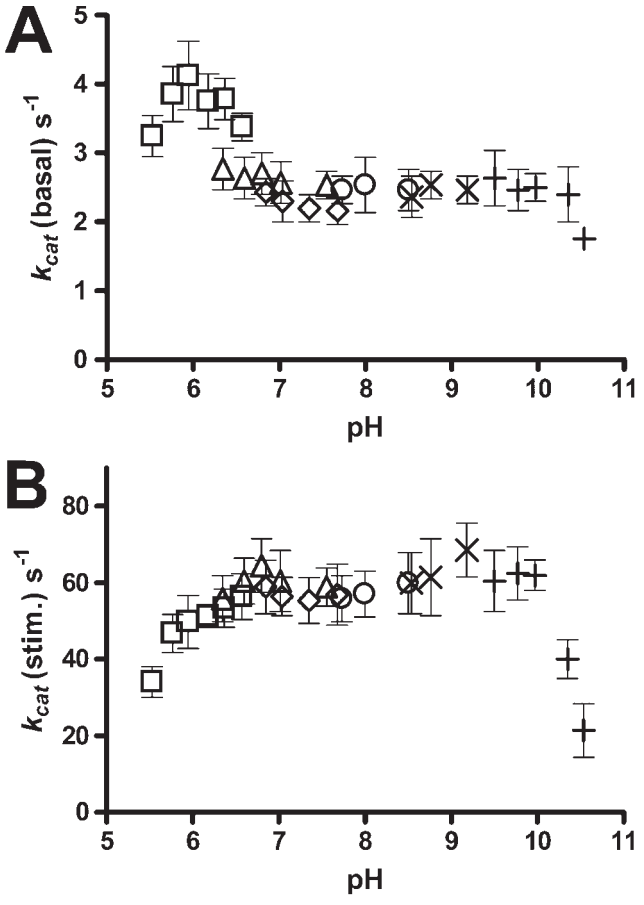

Figure 4. Effect of pH on HCV helicase catalyzed ATP hydrolysis. (**A**) Turnover rate of ATP hydrolysis catalyzed by His–Hel in the absence of nucleic acid as a function of pH. (**B**) Turnover rate of ATP hydrolysis catalyzed by His–Hel in the presence of saturating 2 mM poly(U) RNA. In both (A) and (B), reactions were performed in MES buffer (squares), PIPES buffer (triangles), MOPS buffer (diamonds), TRIS buffer (circles), Tricene buffer (×) or CAPS buffer (+). Average rate constants from four separate determinations are shown with the standard deviations as error bars.

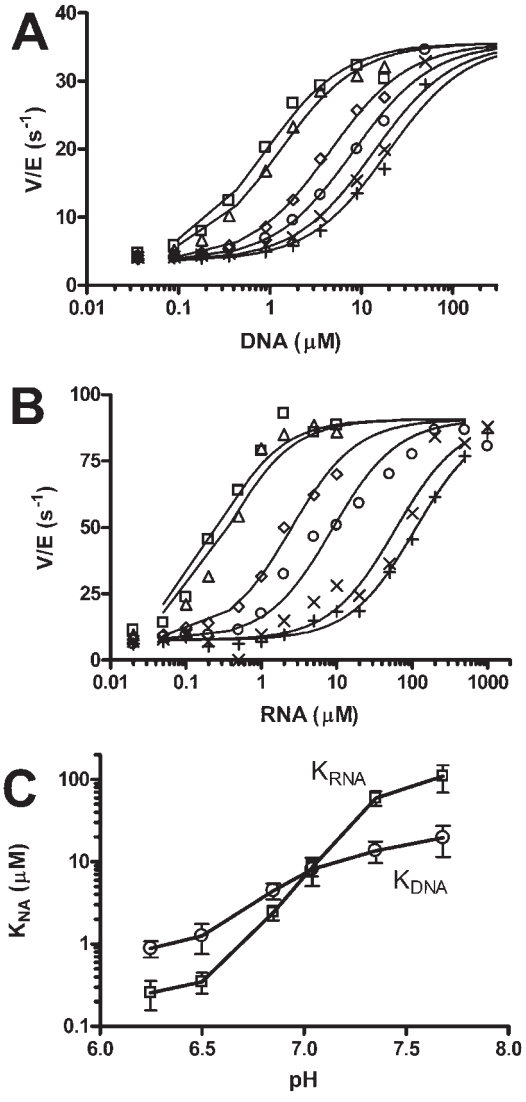

Figure 5. Effect of RNA and DNA on HCV helicase catalyzed ATP hydrolysis at different pH. (**A**) Initial rates of ATP hydrolysis at various concentrations of the ssDNA oligonucleotide dT20. (**B**) Initial rates of ATP hydrolysis at various concentrations of poly(U) RNA (average length 2500 nt). In both (A) and (B), reactions were performed in MOPS buffer at pH 6.25 (squares), pH 6.5 (triangles), pH 6.85 (diamonds), pH 7.04 (circles), pH 7.35 (×) and pH 7.68 (+). The data were fit to Equation 2 to determine the concentration necessary to support a half maximum rate of ATP hydrolysis (K_{NA}). (**C**) Each titration was repeated 2–5 times and the average K_{NA}s determined at each pH for either RNA (squares) or ssDNA (circles) are plotted with the standard deviation shown as error bars.

depends on nucleic acid binding and its release, is highly pH-dependent. A lower K_{NA} suggests that the protein binds nucleic acids more tightly. As pH falls, so does K_{NA}, with the tightest binding occurring in low pH buffers. Both K_{DNA}, measured using a poly(T) oligonucleotide (Figure 5A), and K_{RNA}, measured using poly(U) RNA (Figure 5B), fell dramatically when pH was lowered from 7.5 to 6.5; K_{RNA} was more influenced by pH than K_{DNA} (Figure 5C). K_{RNA} of His–Hel decreased by ~48-fold, while K_{DNA} decreased 20-fold. When the same nucleic acid titrations were repeated with His–NS3–4A, both K_{RNA} and the K_{DNA} again decreased significantly when pH was lowered from 7.5, although values were difficult to precisely measure because ATP hydrolysis catalyzed by the full-length protein was only stimulated ~10-fold (16).

Effect of pH on the interaction between the HCV NS3 and DNA

The above analysis of the effect of pH on HCV helicase catalyzed ATP hydrolysis suggests that nucleic acid binding is highly pH-dependent, and at low pH, RNA and DNA bind more tightly. However, measurements of the kinetic constants, K_{DNA} and K_{RNA}, do not truly reflect the affinity of the protein for DNA or RNA, because they depend not only on nucleic acid equilibrium binding and release, but also on the rates of helicase translocation and ATP hydrolysis. In order to analyze the pH dependence of the interaction between NS3 and nucleic acids directly, the equilibrium dissociation constant (K_D) describing DNA-helicase binding was determined as a function of pH. The assay that was used exploits the ability of DNA to quench the intrinsic protein fluorescence of HCV helicase (14,18,29). To measure the affinity of His–Hel for DNA, His–Hel was titrated with increasing concentrations of a dT20 ssDNA oligonucleotide while monitoring intrinsic protein fluorescence. As shown in Figure 6A, virtually identical results were obtained in all MOPS buffers (pH 6.5–7.68). The resulting K_Ds, which were calculated by fitting the data to Equation 3, varied from 1.2 to 2.9 nM (Figure 6A insert). When the titrations were repeated using the shorter RNA oligonucleotide used in unwinding assays, again only minor differences in K_Ds were observed (data not shown). In both cases, however, there was a slight trend toward weaker binding at high pH, but the K_D values were within experimental error, which encompassed the range of K_Ds obtained from repeat titrations. The data must also be cautiously interpreted because a concentration of protein (>30 nM) much higher than the apparent K_D (<2 nM) was needed to accurately measure intrinsic protein fluorescence, and it is therefore possible that these assays are not sensitive enough to measure differences in binding affinities in this pH range. Nevertheless, the K_Ds obtained from direct binding experiments (Figure 6A) do not directly parallel the K_{NA}s obtained from ATPase assays (Figure 5C).

Why might K_{NA} be pH-dependent if the K_D for helicase and DNA is not pH-dependent? The difference between the two experiments was that when K_{NA} was determined, saturating amounts of ATP were present, whereas the K_D was determined in the absence of ATP. It is possible that ATP affects the pH dependence of DNA binding. To test this hypothesis, the above binding experiments were repeated in the presence of

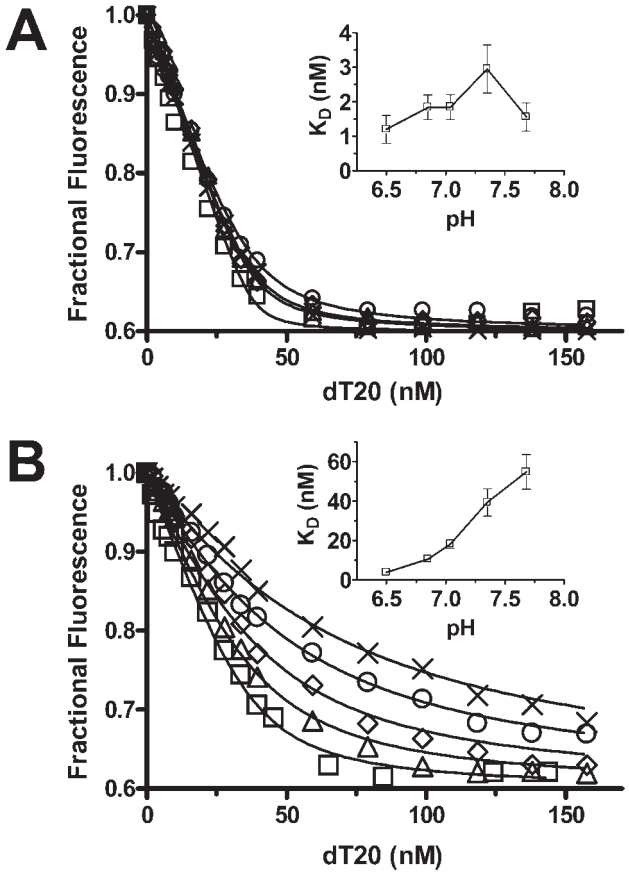

Figure 6. Effect of pH on the interaction between HCV helicase and a DNA oligonucleotide. (**A**) Intrinsic protein fluorescence (extinction 280 nm, emmission 340 nm) of 38 nM His–Hel was measured in the presence of various concentrations of a DNA oligonucleotide (dT20) in MOPS buffers at pH 6.5 (squares), pH 6.85 (triangles), pH 7.04 (diamonds), pH 7.35 (circles) and pH 7.68 (×). The fraction of the fluorescence signal remaining after DNA addition is plotted versus oligonucleotide concentration. (**B**) Titrations in (A) were repeated in the presence of ADP(BeF_3), which was formed by adding 0.1 mM ADP, 0.5 mM BeF_2 and 5 mM NaF to the reaction buffer. Data were fit to Equation 3 using non-linear regression. Each titration was repeated three times and the average K_Ds are plotted versus pH in the inserts. Error bars encompass the range of K_Ds obtained at each pH.

ADP(BeF_3), which was recently shown to bind HCV helicase like a non-hydrolyzable ATP analog (15). As shown in Figure 6B, in higher pH MOPS buffers, a substantially increased amount of DNA was required to quench fluorescence when ADP(BeF_3) was present in the solution. When the data were fit to Equation 3 to determine the dissociation constant, it was clear that K_D increased by a magnitude comparable to that seen in the ATPase assays (compare Figure 5C with Figure 6B insert).

Unfortunately, it was not possible to repeat these titrations with the full-length protein because of added background fluorescence arising from the protease domain (16). Therefore, as a control, these titrations were repeated with two other truncated NS3 helicases, one where the His-tag is placed on the C-terminus (Hel–His), and another with His-tags at both the N- and C- termini (His–Hel–His). It is possible that titration of the histidines caused the increase in DNA affinity. This

is likely not the case, because all fusion proteins were similarly affected by pH increases in the presence of ADP(BeF_3) (data not shown).

Effect of pH on the binding of a Mg^{2+}mantADP(BeF_3) complex to HCV helicase

Based on the above data, it appears that the main reason that the HCV helicase unwinds duplex nucleic acids better at low pH is because it binds more tightly to nucleic acids under low-pH conditions. It is also possible that this activation could be due to better interaction with ATP, but the above kinetic analysis of ATP hydrolysis suggests that neither turnover rate nor K_m is influenced when pH is lowered from 7.5. On the other hand, K_m values may not appropriately measure helicase affinity for ATP because there is yet no direct evidence that HCV helicase and ATP are in a state of rapid equilibrium. Therefore, we decided to examine the effect of pH on the affinity of ATP for HCV helicase using direct binding experiments. Recently, Levin *et al*. (15) showed that FRET could be used to monitor the binding of the fluorescently labeled non-hydrolyzable ATP analog mantADP(BeF_3) to HCV helicase. This is possible because mantADP absorbs light near the tryptophan emission wavelength. FRET can be observed in a HCV helicase–mantADP(BeF_3) complex by exciting the sample at 280 nm while monitoring fluorescence emission at 440 nm. To estimate the affinity of HCV helicase for ATP, the various helicases described here were titrated with mantADP. In each case, no significant difference in the affinity of MantADP(BeF_3) were observed in the various MOPS buffers utilized. As shown in Figure 7A, there was a slight trend toward tighter binding at high pH but these small differences were within experimental error, which includes the range of K_Ds obtained from repeated titrations.

As was originally reported by Levin *et al*. (15), the FRET observed in Figure 7A is dependent absolutely on the presence of BeF_3; mantADP binds the enzyme very weakly. BeF_3 is believed to coordinate like the gamma phosphate of ATP as has been seen in structures of other enzyme such as nucleoside diphosphate kinase (30). When a solution containing mantADP, HCV helicase and NaF is titrated with beryllium, FRET is hyperbolically dependent on beryllium concentration in a manner that a dissociation constant of ~25 μM can be determined (15). We have repeated beryllium titrations with the proteins and buffer described here and again, the binding of beryllium is pH-independent (data not shown). In addition to requiring beryllium, formation of the helicase–mantADP(BeF_3) complex (as determined by FRET), also requires magnesium, which most likely helps position BeF_3 with the phosphates of mantADP. Therefore, we used FRET to examine the affinity of Mg^{2+} in this complex. A solution containing HCV helicase, mantADP, NaF and BeF_3 was titrated with $MgCl_2$, and FRET was recorded. As shown in Figure 7B, Mg^{2+} binds 3.5-fold more weakly when pH is lowered from 7.6 to 6.25. Thus, there may be a subtle effect of pH on ATP binding, but this effect is at least an order of magnitude less than the effect of pH on DNA binding to the helicase. It is possible that the presence of ssDNA could amplify this pH effect on ATP binding. Unfortunately, we could not test this hypothesis because ATP binds less tightly in the presence of DNA, and consequently, no FRET could be observed between helicase and mantADP in the presence of ssDNA.

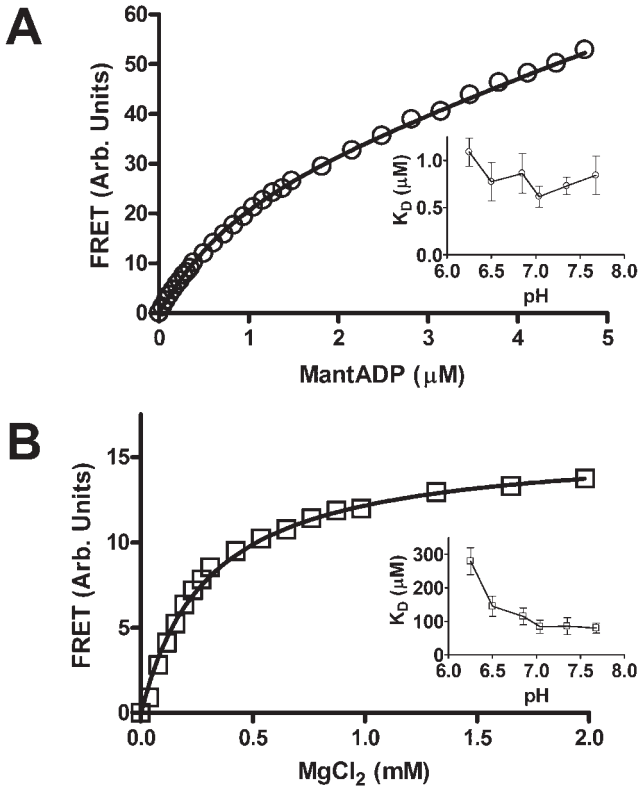

Figure 7. FRET analysis of mantADP(BeF_3) binding to HCV helicase at various pH. (**A**) A solution containing 0.5 μM Hel–His, 5 mM NaF, 0.5 mM BeF_2, 3 mM $MgCl_2$, 25 mM MOPS, pH 7 was titrated with mantADP. FRET was determined by exciting the sample at 280 nm and monitoring fluorescence emitted at 443 nm. Data were fit to Equation 4 using non-linear regression to determine a K_D. (**B**) A solution containing 0.5 μM Hel–His, 5 mM NaF, 0.5 mM BeF_2, 25 mM MOPS, pH 6.25, 2 μM mantADP was titrated with $MgCl_2$. FRET was measured as in (A). Data were fit to Equation 5 to determine K_D. The inserts show the average resulting K_Ds when the titrations were repeated twice in various pH MOPS buffers.

DISCUSSION

Although the precise role of HCV helicase in viral replication is not clear, the protein most likely unwinds base-paired viral RNA during translation or replication. Our results suggest that this activity might be very sensitive to changes in local cellular pH. The fact that low-pH activation of helicase is conserved among HCV genotypes also highlights its importance. The three Hel–His enzymes studied here share only ~85% of their amino acids and none of the dozens of amino acid differences influence the protein's pH profile. Furthermore, although it is possible that the interaction of HCV helicase with other viral or cellular proteins will abrogate its low-pH requirement, the presence of the protease domain and the NS4A cofactor only somewhat enhances RNA unwinding at neutral pH. Below, we speculate on how the virus might exploit the pH sensitivity of the HCV helicase, and how the data presented here could help to explain how HCV helicase moves along RNA molecules.

It is usual for cellular pH changes to play key roles in viral lifecycles. For example, when influenza virus enters a cell through endocytosis, it is activated only when pH is reduced in late endosomes. When this happens, the viral M2 protein allows protons to pass into the virion, where the change in pH

activates the influenza replication complex. The antiviral drug amantadine binds the M2 protein to block proton flow and halt influenza replication. Although there is no direct evidence yet that HCV enters cells via a similar pathway, perhaps it is not simply a coincidence that amantadine has shown some clinical efficacy in HCV patients (31).

Since there is no way yet to cultivate HCV *in vitro* or in any organism other than the chimpanzee, the role of pH changes in HCV replication is not examined easily. Studies with HCV replicons have nevertheless provided some evidence that our *in vitro* results might be relevant *in vivo*. When HCV RNA is translated in cultured cells, NS3 assembles with other viral non-structural proteins on the endoplasmic reticulum (ER) (32). HCV proteins expressed from replicons modify ER membranes to create a web (33,34), which protects viral RNA from nuclease digestion (35). Similar to related ssRNA viruses, this membranous web complex might then progress through the Golgi apparatus to eventually bud from the cell. The pH in the ER is typically ~7.2, the pH of the Golgi is ~6.4 (36) and HCV replication complexes have been detected in both these organelles (37,38). Our data suggest that HCV helicase might be most active in the Golgi, where it might unwind duplex RNA to package one strand in the virion. It is also interesting to note that, like the influenza M2 protein, HCV p7 protein can form an ion channel in an artificial bilayer system (39), which can be blocked by the drug amantadine (40).

It should also be noted that the pH optimum of the NS3 protease is quite different from that of the helicase. The full-length NS3–4A complex studied here has an optimal protease activity at pH 8.0, and pH changes in either direction result in significant loss of protease activity (41,42). It is possible that even though the protease and helicase functions reside within the same protein, each is active at a different stage of the HCV replication cycle depending on the local pH environment. In a similar manner, we also note here that RNA unwinding is more sensitive to pH increases than DNA unwinding. This means that NS3 effectively unwinds DNA under conditions where it is unable to unwind RNA. It is noteworthy that under certain conditions, the NS3 protein has been detected in the nucleus (43) where it could influence host gene expression (44). Our data reveal that a low-pH environment would not be necessary for HCV helicase to unwind host DNA.

The molecular basis of HCV helicase low-pH activation can be explained by the model described in Figure 8, which proposes that the protein exists in two basic conformations and the transition between the two states is regulated by ATP binding. When ATP is absent, the protein tightly binds RNA, and when

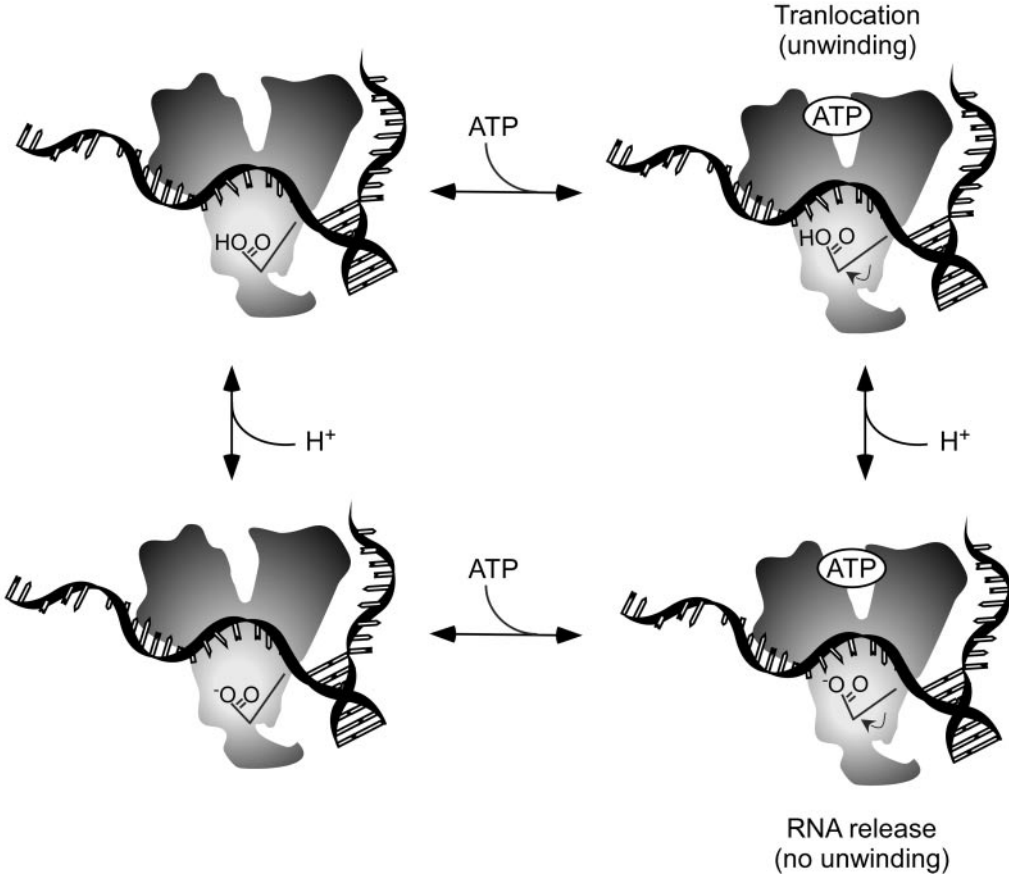

Figure 8. Acid activation of the HCV helicase. HCV helicase unwinds RNA (and DNA) near pH 6.5 with the enzyme reaching ~50% activity at pH 7. Between pH 6.5 and 7.5, the affinity of an enzyme–ATP complex for RNA increases by almost 100-fold. In this range, the affinity of the enzyme for ATP or ssDNA varies <3-fold. This simple model explains the data by suggesting that an acidic side chain, with a pK_a near 7, which is not in contact with ssDNA in the absence of ATP, rotates near RNA upon ATP binding. At low pH, the protonated polar side chain would repel RNA enough to allow translocation and processive unwinding. At higher pH, the negatively charged side chain would repel RNA so strongly that RNA is released and the processive reaction is terminated. Although only a single acidic side chain is noted on the diagram, it is clearly possible that multiple acidic residues work in concert to produce this effect.

ATP is present, the protein binds more loosely and slides along DNA. Our data reveal that at low pH the helicase–ATP complex binds nucleic acids significantly (50-fold) more tightly than it does at higher pH. This suggests that an ionizable side chain (or several side chains) with a pK_a of ~7, which is normally not in contact with RNA in the absence of ATP, rotates into the RNA binding cleft upon ATP binding. In Figure 8, this is diagramed as the rotation of an acidic side chain, which in its negatively charged state would repel the protein from the phosphate backbone of RNA (or DNA). It is also possible that a basic amino acid that is neutral above pH 7 gains a proton, and is subsequently positively charged at low pH. We chose to depict a negatively charged amino acid because a positively charged residue might attract the RNA and prevent the helicase from translocating. Rotation of a polar uncharged residue, on the other hand might still provide enough dipole repulsion to push the helicase along RNA. Such a propulsion mechanism would also explain the propensity of HCV helicase to move only in a 3′ to 5′ direction along a single-stranded nucleic acid chain (45).

The model in Figure 8 depicts the HCV helicase moving along RNA as a monomer for simplicity, and because there is no direct structural evidence yet that the protein forms a dimer or higher order oligomer alone or in the presence of short oligonucleotides (9,46). It should be noted, however, that there is accumulating biochemical evidence that several HCV helicase monomers assemble on nucleic acid chains longer than 10 bases (15,16,47,48). We envision that the other protein subunits in such a helicase assembly could act to catch RNA that is inadvertently released upon ATP binding. A similar idea was recently used by Levin *et al*. (49) to explain the ability of HCV helicase to unwind substrates more efficiently with longer ssDNA tails better than similar substrates with short tails.

Any protein could conceivably use the method depicted in Figure 8 to travel along a nucleic acid template. By rotating negatively charged amino acids toward the negatively charged backbone of DNA or RNA, the resulting electrostatic repulsion could propel the protein. If the protein is tightly clamped to DNA, then this propulsion mechanism could be used effectively at any pH where the acidic residues are negatively charged. Since there are no evidences that HCV helicase encircles RNA like the so-called 'ring' helicases (50), it is possible that this propulsion technique only works well for HCV helicase at lower pH, where the force would be smaller. Although this 'propulsion-by-repulsion' model is speculative, it is simple and predictive. If the critical negatively charged residues are changed, then both enzyme-catalyzed unwinding and its pH profile should be altered. We intend to test this model using site-directed mutagenesis to alter charged amino acids that are located in the RNA binding cleft of the HCV helicase.

ACKNOWLEDGEMENTS

We thank Baohua Gu for the gift of purified His–NS3–4A protein and Fred Jaffe and Ruth Gallagher for their valuable technical assistance. This work was supported by a Liver Scholar Award from the American Liver Foundation and National Institutes of Health grant AI052395.

REFERENCES

1. Frick,D.N. (2004) The hepatitis C virus replicase: insights into RNA-dependent RNA replication and prospects for rational drug design. *Curr. Org. Chem.*, **8**, 223–241.
2. Kolykhalov,A.A., Mihalik,K., Feinstone,S.M. and Rice,C.M. (2000) Hepatitis C virus-encoded enzymatic activities and conserved RNA elements in the 3′ nontranslated region are essential for virus replication *in vivo*. *J. Virol.*, **74**, 2046–2051.
3. Lamarre,D., Anderson,P.C., Bailey,M., Beaulieu,P., Bolger,G., Bonneau,P., Bos,M., Cameron,D.R., Cartier,M., Cordingley,M.G. *et al*. (2003) An NS3 protease inhibitor with antiviral effects in humans infected with hepatitis C virus. *Nature*, **426**, 186–189.
4. Silverman,E., Edwalds-Gilbert,G. and Lin,R.J. (2003) DExD/H-box proteins and their partners: helping RNA helicases unwind. *Gene*, **312**, 1–16.
5. Gorbalenya,A.E. and Koonin,E.V. (1993) Helicases: amino acid sequence comparisons and structure–function relationships. *Curr. Opin. Struct. Biol.*, **3**, 419–429.
6. Sung,P., Prakash,L., Matson,S.W. and Prakash,S. (1987) RAD3 protein of *Saccharomyces cerevisiae* is a DNA helicase. *Proc. Natl Acad. Sci. USA*, **84**, 8951–8955.
7. Lehmann,A.R. (2001) The xeroderma pigmentosum group D (XPD) gene: one gene, two functions, three diseases. *Genes Dev.*, **15**, 15–23.
8. Yao,N., Hesson,T., Cable,M., Hong,Z., Kwong,A.D., Le,H.V. and Weber,P.C. (1997) Structure of the hepatitis C virus RNA helicase domain. *Nature Struct. Biol.*, **4**, 463–467.
9. Kim,J.L., Morgenstern,K.A., Griffith,J.P., Dwyer,M.D., Thomson,J.A., Murcko,M.A., Lin,C. and Caron,P.R. (1998) Hepatitis C virus NS3 RNA helicase domain with a bound oligonucleotide: the crystal structure provides insights into the mode of unwinding. *Structure*, **6**, 89–100.
10. Cho,H.S., Ha,N.C., Kang,L.W., Chung,K.M., Back,S.H., Jang,S.K. and Oh,B.H. (1998) Crystal structure of RNA helicase from genotype 1b hepatitis C virus. A feasible mechanism of unwinding duplex RNA. *J. Biol. Chem.*, **273**, 15045–15052.
11. Yao,N., Reichert,P., Taremi,S.S., Prosise,W.W. and Weber,P.C. (1999) Molecular views of viral polyprotein processing revealed by the crystal structure of the hepatitis C virus bifunctional protease-helicase. *Struct. Fold. Des.*, **7**, 1353–1363.
12. Liu,D., Wang,Y.S., Gesell,J.J. and Wyss,D.F. (2001) Solution structure and backbone dynamics of an engineered arginine-rich subdomain 2 of the hepatitis C virus NS3 RNA helicase. *J. Mol. Biol.*, **314**, 543–561.
13. Liu,D., Windsor,W.T. and Wyss,D.F. (2003) Double-stranded DNA-induced localized unfolding of HCV NS3 helicase subdomain 2. *Protein Sci.*, **12**, 2757–2767.
14. Lam,A.M., Keeney,D. and Frick,D.N. (2003) Two novel conserved motifs in the hepatitis C virus NS3 protein critical for helicase action. *J. Biol. Chem.*, **278**, 44514–44524.
15. Levin,M.K., Gurjar,M.M. and Patel,S.S. (2003) ATP binding modulates the nucleic acid affinity of hepatitis C virus helicase. *J. Biol. Chem.*, **278**, 23311–23316.
16. Frick,D.N., Rypma,R.S., Lam,A.M. and Gu,B. (2004) The nonstructural protein 3 protease/helicase requires an intact protease domain to efficiently unwind duplex RNA. *J. Biol. Chem.*, **279**, 1269–1280.
17. Lam,A.M.I., Keeney,D., Eckert,P.Q. and Frick,D.N. (2003) Hepatitis C virus NS3 ATPases/helicases from different genotypes exhibit variations in enzymatic properties. *J. Virol.*, **77**, 3950–3961.
18. Levin,M.K. and Patel,S.S. (2002) Helicase from hepatitis C virus, energetics of DNA binding. *J. Biol. Chem.*, **277**, 29377–29385.
19. Gwack,Y., Kim,D.W., Han,J.H. and Choe,J. (1996) Characterization of RNA binding activity and RNA helicase activity of the hepatitis C virus NS3 protein. *Biochem. Biophys. Res. Commun.*, **225**, 654–659.
20. Gallinari,P., Brennan,D., Nardi,C., Brunetti,M., Tomei,L., Steinkuhler,C. and De Francesco,R. (1998) Multiple enzymatic activities associated with recombinant NS3 protein of hepatitis C virus. *J. Virol.*, **72**, 6758–6769.
21. Wardell,A.D., Errington,W., Ciaramella,G., Merson,J. and McGarvey,M.J. (1999) Characterization and mutational analysis of the helicase and NTPase activities of hepatitis C virus full-length NS3 protein. *J. Gen. Virol.*, **80**, 701–709.
22. Du,M.X., Johnson,R.B., Sun,X.L., Staschke,K.A., Colacino,J. and Wang,Q.M. (2002) Comparative characterization of two DEAD-box RNA helicases in superfamily II: human translation-initiation factor 4A

and hepatitis C virus non-structural protein 3 (NS3) helicase. *Biochem. J.*, **363**, 147–155.
23. Tai,C.L., Chi,W.K., Chen,D.S. and Hwang,L.H. (1996) The helicase activity associated with hepatitis C virus nonstructural protein 3 (NS3). *J. Virol.*, **70**, 8477–8484.
24. Gwack,Y., Kim,D.W., Han,J.H. and Choe,J. (1997) DNA helicase activity of the hepatitis C virus nonstructural protein 3. *Eur. J. Biochem.*, **250**, 47–54.
25. Suzich,J.A., Tamura,J.K., Palmer-Hill,F., Warrener,P., Grakoui,A., Rice,C.M., Feinstone,S.M. and Collett,M.S. (1993) Hepatitis C virus NS3 protein polynucleotide-stimulated nucleoside triphosphatase and comparison with the related pestivirus and flavivirus enzymes. *J. Virol.*, **67**, 6152–6158.
26. Morgenstern,K.A., Landro,J.A., Hsiao,K., Lin,C., Gu,Y., Su,M.S. and Thomson,J.A. (1997) Polynucleotide modulation of the protease, nucleoside triphosphatase, and helicase activities of a hepatitis C virus NS3–NS4A complex isolated from transfected COS cells. *J. Virol.*, **71**, 3767–3775.
27. Kyono,K., Miyashiro,M. and Taguchi,I. (2003) Characterization of ATPase activity of a hepatitis C virus NS3 helicase domain, and analysis involving mercuric reagents. *J. Biochem. (Tokyo)*, **134**, 505–511.
28. Pang,P.S., Jankowsky,E., Planet,P.J. and Pyle,A.M. (2002) The hepatitis C viral NS3 protein is a processive DNA helicase with cofactor enhanced RNA unwinding. *EMBO J.*, **21**, 1168–1176.
29. Preugschat,F., Averett,D.R., Clarke,B.E. and Porter,D.J.T. (1996) A steady-state and pre-steady-state kinetic analysis of the NTPase activity associated with the hepatitis C virus NS3 helicase domain. *J. Biol. Chem.*, **271**, 24449–24457.
30. Xu,Y.W., Morera,S., Janin,J. and Cherfils,J. (1997) AlF3 mimics the transition state of protein phosphorylation in the crystal structure of nucleoside diphosphate kinase and MgADP. *Proc. Natl Acad. Sci. USA*, **94**, 3579–3583.
31. Teuber,G., Pascu,M., Berg,T., Lafrenz,M., Pausch,J., Kullmann,F., Ramadori,G., Arnold,R., Weidenbach,H., Musch,E. *et al.* (2003) Randomized, controlled trial with IFN-alpha combined with ribavirin with and without amantadine sulphate in non-responders with chronic hepatitis C. *J. Hepatol.*, **39**, 606–613.
32. Wolk,B., Sansonno,D., Krausslich,H.G., Dammacco,F., Rice,C.M., Blum,H.E. and Moradpour,D. (2000) Subcellular localization, stability, and trans-cleavage competence of the hepatitis C virus NS3-NS4A complex expressed in tetracycline-regulated cell lines. *J. Virol.*, **74**, 2293–2304.
33. Mottola,G., Cardinali,G., Ceccacci,A., Trozzi,C., Bartholomew,L., Torrisi,M.R., Pedrazzini,E., Bonatti,S. and Migliaccio,G. (2002) Hepatitis C virus nonstructural proteins are localized in a modified endoplasmic reticulum of cells expressing viral subgenomic replicons. *Virology*, **293**, 31–43.
34. Egger,D., Wolk,B., Gosert,R., Bianchi,L., Blum,H.E., Moradpour,D. and Bienz,K. (2002) Expression of hepatitis C virus proteins induces distinct membrane alterations including a candidate viral replication complex. *J. Virol.*, **76**, 5974–5984.
35. Miyanari,Y., Hijikata,M., Yamaji,M., Hosaka,M., Takahashi,H. and Shimotohno,K. (2003) Hepatitis C virus non-structural proteins in the probable membranous compartment function in viral genome replication. *J. Biol. Chem.*, **278**, 50301–50308.
36. Wu,M.M., Llopis,J., Adams,S., McCaffery,J.M., Kulomaa,M.S., Machen,T.E., Moore,H.P. and Tsien,R.Y. (2000) Organelle pH studies using targeted avidin and fluorescein-biotin. *Chem. Biol.*, **7**, 197–209.
37. Kim,J.E., Song,W.K., Chung,K.M., Back,S.H. and Jang,S.K. (1999) Subcellular localization of hepatitis C viral proteins in mammalian cells. *Arch. Virol.*, **144**, 329–343.
38. Serafino,A., Valli,M.B., Andreola,F., Crema,A., Ravagnan,G., Bertolini,L. and Carloni,G. (2003) Suggested role of the Golgi apparatus and endoplasmic reticulum for crucial sites of hepatitis C virus replication in human lymphoblastoid cells infected *in vitro*. *J. Med. Virol.*, **70**, 31–41.
39. Pavlovic,D., Neville,D.C., Argaud,O., Blumberg,B., Dwek,R.A., Fischer,W.B. and Zitzmann,N. (2003) The hepatitis C virus p7 protein forms an ion channel that is inhibited by long-alkyl-chain iminosugar derivatives. *Proc. Natl Acad. Sci. USA*, **100**, 6104–6108.
40. Griffin,S.D., Beales,L.P., Clarke,D.S., Worsfold,O., Evans,S.D., Jaeger,J., Harris,M.P. and Rowlands,D.J. (2003) The p7 protein of hepatitis C virus forms an ion channel that is blocked by the antiviral drug, Amantadine. *FEBS Lett.*, **535**, 34–38.
41. Taremi,S.S., Beyer,B., Maher,M., Yao,N., Prosise,W., Weber,P.C. and Malcolm,B.A. (1998) Construction, expression, and characterization of a novel fully activated recombinant single-chain hepatitis C virus protease. *Protein Sci.*, **7**, 2143–2149.
42. Sali,D.L., Ingram,R., Wendel,M., Gupta,D., McNemar,C., Tsarbopoulos,A., Chen,J.W., Hong,Z., Chase,R., Risano,C. *et al.* (1998) Serine protease of hepatitis C virus expressed in insect cells as the NS3/4A complex. *Biochemistry*, **37**, 3392–3401.
43. Muramatsu,S., Ishido,S., Fujita,T., Itoh,M. and Hotta,H. (1997) Nuclear localization of the NS3 protein of hepatitis C virus and factors affecting the localization. *J. Virol.*, **71**, 4954–4961.
44. Sakamuro,D., Furukawa,T. and Takegami,T. (1995) Hepatitis C virus nonstructural protein NS3 transforms NIH 3T3 cells. *J. Virol.*, **69**, 3893–3896.
45. Morris,P.D., Byrd,A.K., Tackett,A.J., Cameron,C.E., Tanega,P., Ott,R., Fanning,E. and Raney,K.D. (2002) Hepatitis C virus NS3 and simian virus 40 T antigen helicases displace streptavidin from 5′-biotinylated oligonucleotides but not from 3′- biotinylated oligonucleotides: evidence for directional bias in translocation on single-stranded DNA. *Biochemistry*, **41**, 2372–2378.
46. Porter,D.J., Short,S.A., Hanlon,M.H., Preugschat,F., Wilson,J.E., Willard,D.H.,Jr and Consler,T.G. (1998) Product release is the major contributor to k_{cat} for the hepatitis C virus helicase-catalyzed strand separation of short duplex DNA. *J. Biol. Chem.*, **273**, 18906–18914.
47. Levin,M.K. and Patel,S.S. (1999) The helicase from hepatitis C virus is active as an oligomer. *J. Biol. Chem.*, **274**, 31839–31846.
48. Khu,Y.L., Koh,E., Lim,S.P., Tan,Y.H., Brenner,S., Lim,S.G., Hong,W.J. and Goh,P.Y. (2001) Mutations that affect dimer formation and helicase activity of the hepatitis C virus helicase. *J. Virol.*, **75**, 205–214.
49. Levin,M.K., Wang,Y.H. and Patel,S.S. (2004) The functional interaction of the hepatitis C virus helicase molecules is responsible for unwinding processivity. *J. Biol. Chem.*, **279**, 26005–26012.
50. Patel,S.S. and Picha,K.M. (2000) Structure and function of hexameric helicases. *Annu. Rev. Biochem.*, **69**, 651–697.